occurs via GLY2 (i.e., GLY1 $\rightarrow$ GLY2 $\rightarrow$ GLY12) rather than GLY9, on the basis of relative rate constants presented in Table VIII. Equilibrium reversals, shown by calculating equilibrium constants (Table VIII), with increasing temperatures are observed for two different equilibria: GLY1 $\leftrightarrow$ GLY2 and GLY9 $\leftrightarrow$ GLY16M. The former is explained by the large equilibrium partition function of GLY2 relative to GLY1 (caused, again, by the large vibrational entropy of GLY2), which dominates the equilibrium constants as the difference in relative energies approaches zero. The latter is due to a reversal of stability of GLY9 and GLY16M as the temperature is increased (Figure 1).

Two main points emerge from the comparison of this with other studies. One is that conformational potential energy maps[1,7] have to be rather refined to locate all minima on the glycine PES. The second is that one conformation (GLY3, Scheme I) is a transition state on the electronic PES, but that the electronic barrier is so small that the vibrational energies of the normal modes are sufficient to overcome this barrier. Thus, this study suggests that GLY3 is the conformational average of the free internal interconversion between GLY16 and its mirror image, and hence observed in microwave spectra.[2,3]

**Acknowledgment**. This work was supported in part by a grant from the Petroleum Research Fund, administered by the American Chemical Society. Computer time was made available by the North Dakota State University Computer Center on its IBM 3090/200E, obtained via a joint study agreement with IBM. Additional calculations were carried out on a DECstation 3100 and a VAXstation 3200, both funded by a grant from the National Science Foundation (CHE86-40771). We would like to thank Nikita Matsunaga for drawing our attention to Dr. Ramek's paper. Helpful discussions with Dr. Michael Ramek, Dr. Walter Stevens, and Dr. Donald Truhlar are gratefully acknowledged.

**Registry No.** Gly, 56-40-6.

**Supplementary Material Available:** Tables listing bond lengths, bond angles, and dihedral angles of the eight $C_s$ conformers of glycine, the four $C_1$ minima of glycine, and GLYTS1-15 (4 pages). Ordering information is given on any current masthead page.

---

# Structures and Bonding of Group IV Sulfur and Oxygen Propellane Derivatives

**Kiet A. Nguyen, Marshall T. Carroll,[†] and Mark S. Gordon***

*Contribution from the Department of Chemistry, North Dakota State University, Fargo, North Dakota 58105-5516.* *Received March 25, 1991*

**Abstract:** The RHF, ROHF, and GVB structures and energetics of group IV 2,4,5-trioxa[1.1.1]metallapropellanes, 2,4,5-trithia[1.1.1]metallapropellanes, and their bicyclopentane analogues have been determined from ab initio molecular orbital theory by using both the 6-31G(d) basis set for all-electron calculations and the valence basis set with effective core potentials (ECP) developed by Stevens, Basch, and Krauss. Although they have extremely short bridgehead distances, these species possess fairly large natural orbital occupation numbers in the lowest unoccupied molecular orbitals, indicating significant diradical character. Structures and other properties determined by ECP calculations are in good agreement with the 6-31G(d) all-electron calculations.

## I. Introduction

Considerable attention has been given to group IV propellanes (**1**) (M = C, Si, Ge, Sn) and their derivatives in an effort to understand the nature of the bridgehead bonds ($M_b$–$M_b$). Despite a highly strained "inverted" tetrahedral arrangement at the bridgehead atoms, the simplest propellane (M = C) was successfully synthesized by Wiberg and co-workers.[1] This reactive compound (reacting rapidly with various reagents at the bridgehead positions[2]), with an experimental $M_b$–$M_b$ bridgehead distance (1.60 Å)[3] that is slightly longer than the peripheral $M_b$–$M_p$ bond (1.52 Å) and much shorter than the bridgehead bond (1.84 Å)[4] in bicyclo[1.1.1]pentane (**2**), has been a subject of discussion among both experimentalists[2,3,5] and theoreticians.[1,6,7-12] The silicon,[6,13-15] germanium[15,16a] and tin[15] analogues have also been theoretically investigated. Experimentally, pentasila[1.1.1]propellane is not known, although a derivative (1,3-bis(4-*tert*-butyl-2,6-diisopropylphenyl)-2,2,4-tetraisopropylbicyclo[1.1.1]pentasilane) of bicyclo[1.1.1]pentasilane has been synthesized recently.[16b] For germanium, neither the bicyclo form (**2**) nor the propellane form (**1**) has been experimentally observed.

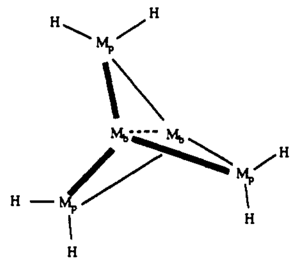

**1** $D_{3h}$

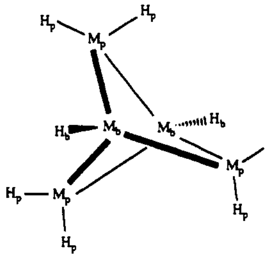

**2** $D_{3h}$

Recently, an investigation of the structure and bonding of pentastanna[1.1.1]propellane and the analogues in group IV has been carried out this laboratory with use of the 3-21G(d) basis set and two different sets of effective core potentials developed by Stevens, Basch, and Krauss (SBK) and Wadt and Hay (WH). The singlet states were investigated at the restricted Hartree–Fock

---

[†] Natural Sciences and Engineering Council of Canada Postdoctoral Fellow.

(1) Wiberg, K. B.; Bader, R. F. W.; Lau, C. D. H. *J. Am. Chem. Soc.* **1987**, *109*, 985.
(2) Wiberg, K. B.; Waddell, S. T. *J. Am. Chem. Soc.* **1990**, *112*, 2194.
(3) (a) Wiberg, K. B.; Walker, F. H. *J. Am. Chem. Soc.* **1982**, *104*, 5239. (b) Wiberg, K. B.; Dailey, W. P.; Walker, F. H.; Waddell, S. T.; Crocker, L. S.; Newton, M. D. *J. Am. Chem. Soc.* **1985**, *107*, 7247.
(4) Wiberg, K. B.; Wendoloski, J. J. *J. Am. Chem. Soc.* **1982**, *104*, 5679.
(5) Wiberg, K. B. *Chem. Rev.* **1989**, *89*, 975.
(6) Schleyer, P. v. R.; Janoschek, R. *Angew. Chem., Int. Ed. Engl.* **1987**, *26*, 1267.
(7) Stohrer, W. D.; Hoffmann, R. *J. Am. Chem. Soc.* **1972**, *94*, 779.
(8) Newton, M. D.; Schulman, J. M. *J. Am. Chem. Soc.* **1972**, *94*, 773.
(9) Jackson, J. E.; Allen, L. C. *J. Am. Chem. Soc.* **1984**, *106*, 591.

0002-7863/91/1513-7924$02.50/0

(RHF) and at the two-configuration self-consistent-field (TCSCF) levels of theory, while the triplet state was analyzed by using the unrestricted Hartree–Fock (UHF) method.[15] The calculated structure of **1** (M = Sn) is consistent with the X-ray crystal structure of 2,2,4,4,5,5-hexakis(2,6-diethylphenyl)pentastanna-[1.1.1]propellane.[15,16c] The RHF/3-21G(d) distance between the bridgehead atoms in **1** (3.463 Å) is much longer than that between the bridgehead and peripheral tin atoms (2.876 Å) and essentially the same as the corresponding $M_b$–$M_b$ distance in **2**. Similarly, the X-ray bridgehead distance ($M_b$–$M_b$) of 3.367 Å of 2,2,4,4,5,5-hexakis(2,6-diethylphenyl)pentastanna[1.1.1]propellane is almost identical with that of its pentastannabicyclo[1.1.1]-pentane analogue ($M_b$–$M_b$ = 3.361 Å).[15,16c] Thus, the experimental and theoretical evidence places the existence of a bridgehead ($M_b$–$M_b$) bond in **1** in doubt when M $\neq$ C. It is interesting that TCSCF calculations for **1** show only a slight increase in diradical character upon going from M = C to Sn. Furthermore, localization of the valence molecular orbitals with the method developed by Foster and Boys[17] gives rise to localized $M_b$–$M_b$ orbitals for all four parent [1.1.1]propellane species (M = C, Si, Ge, Sn). Although no *bond critical point*[12] (a saddle point in the total electron density indicating the existence of a bond between two atoms in a molecule) has been located between the bridgehead atoms for the [1.1.1]metallapropellane systems ($M_b$ = $M_p$ = Si, Ge, Sn), slight differences in the charge densities of these systems can affect the absence or presence of $M_b$–$M_b$ bond critical points in these species.[15] The electron charge density surfaces for these systems, therefore, are very flat, especially around the bridgehead regions. The existence of $M_b$–$M_b$ bond orbitals for $M_b$ = $M_p$ = Si, Ge, or Sn, despite the absence of bond critical points, supports this notion. This suggests that changes in the nature of the peripheral groups might increase or decrease the strengths of the $M_b$–$M_b$ bonding interactions in **1**.

Accordingly, Nagase[13,16a] and others[10] have suggested that substitution of more electronegative groups (oxygen, $CH_2$ groups) at the peripheral positions could stabilize the central $M_b$–$M_b$ interaction for M = Si and Ge. Ab initio calculations for the oxygen derivatives of Si and Ge propellanes (**3**) and bicyclopentanes (**4**), with M = Si, Ge and L = O, have been performed[16a,b] with RHF/6-31G(d) and RHF/3-21G(d) wave functions. For Si, M–M distances in *both* **3** (2.060 Å) and **4** (2.089 Å) are predicted to be extremely short compared to the $M_b$–$M_b$ distance (2.719 Å) of **1** (M = Si) and the $M_b$–$M_b$ distance (2.915 Å) in **2** (M = Si), calculated at the same level of theory.[4] Contractions of similar magnitude are found for M = Ge where RHF/3-21G(d) predicts the bridgehead distance in **3** to be 0.623 Å shorter than that in **1** (2.883 Å) and the bridgehead distance in **4** to be 0.803 Å shorter than that in **2** (3.025 Å).[5] These results were taken as evidence that electronegative substitution at the peripheral centers does indeed stabilize the bridgehead bond and therefore the [1.1.1]propellanes as well. Similar trends have been found for $M_2C_3H_6$ and $M_2C_3H_8$ (M = Si), where the $MH_2$ groups in **1** and **2** are replaced by the more electronegative $CH_2$ groups.[10] To date, no calculations have been reported on the oxapropellane derivatives (**3** and **4**) with M = C and Sn. To our knowledge, neither the group IV 3,4,5-trioxa[1.1.1]propellanes **3** nor their bicyclopentane analogues **4** ($M_b$ = C, Si, Ge, and Sn) have been observed experimentally. Other related compounds that have been synthesized are $[Sn(OtBu)_3Tl]$[16d] **3** (M = Sn and Tl, L = OtBu) and $[Sn(OtBu)_3In]$[16e] **3** (M = Sn and In, L = OtBu).

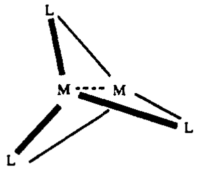

**3** $D_{3h}$

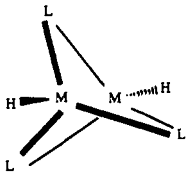

**4** $D_{3h}$

Although the extremely short distances between the central bridgehead atoms in compounds **3** and **4** may be an indication of the existence of a bond, shorter distances do not always correspond to stable bonding interactions.[18] Likewise, significant bonding interactions can occur between atoms separated by long internuclear distances.[15,19a] It is significant in this regard that substitution of L = O leads to a large decrease in the $M_b$–$M_b$ distance in *both* **3** and **4**, since one does not expect the bridgehead atoms to be bonded in the latter. Furthermore, in view of the unusual nature of the bonding in [1.1.1]propellanes and their derivatives, the importance of a multiconfigurational description of the wave function must be assessed. This has been done previously for the parent compounds **1** and **2**,[15] but not for the derivatives of **3** and **4**. Therefore, multiconfigurational wave functions are used in the present paper to probe the nature of the bridgehead interaction. Here, we report results of the second, third, fourth, and fifth period group IV 2,4,5 trioxa[1.1.1]propellane and 2,4,5-trithia[1.1.1]propellane derivatives, as well as their [1.1.1]bicyclopentane analogues. That is, M = C, Si, Ge, Sn and L = O, S. The all-electron results for $Si_2O_3$ and $H_2Si_2O_3$ have recently been presented in the context of other SiO compounds[19b] but are included here for comparison to other propellanes and bicyclopentanes.

## II. Computational Approach

For carbon and silicon, structures were determined with the 6-31G(d) basis set[20] with use of analytical energy gradients with restricted Hartree-Fock[21] (RHF) and restricted open-shell Hartree-Fock[22] (ROHF) wave functions for closed-shell singlets and open-shell triplets, respectively. In addition, TCSCF[23] calculations have been carried out on the singlets to ascertain the diradical character in these compounds; such calculations have been shown to be useful in characterizing the nature of the bridgehead bonds in propellanes.[6,15,19b] Quantitative measurement of the diradical character is given by the CI orbital coefficients. The natural orbital occupation number (NOON) is defined as twice the square of the CI coefficient. In our TCSCF, the highest occupied molecular orbital (HOMO) and the lowest unoccupied molecular orbital (LUMO) are included in the active space. Effective core potential (ECP[24]) calculations (with the SBK basis set[25]) at the RHF, ROHF, and TCSCF levels were also carried out with use of the same d orbital exponents as in the all-electron calculations. Structures were verified as minima by their positive definite hessians (matrices of energy second derivatives), obtained analytically for all-electron calculations and from finite differences of the analytically determined gradients for ECP calculations. These ab initio electronic structure calculations were performed with the GAMESS[26] quantum chemistry program.

---

(10) Kitchen, D. B.; Jackson, J. E.; Allen, L. C. *J. Am. Chem. Soc.* **1990**, *112*, 3408.

(11) Epiotis, N. D. *J. Am. Chem. Soc.* **1984**, *106*, 3170.

(12) Bader, R. F. W.; Nguyen-Dang, T. T.; Tal, Y. *Rep. Prog. Phys.* **1981**, *44*, 893.

(13) (a) Nagase, S.; Kudo, T. *Organometallics* **1987**, *6*, 2456. (b) Nagase, S.; Kudo, T.; Kurakake, T. *J. Chem. Soc., Chem. Commun.* **1988**, 1063.

(14) Schoeller, W. W.; Dabisch, T.; Busch, T. *Inorg. Chem.* **1987**, *26*, 4383.

(15) Gordon, M. S.; Nguyen, K. A.; Carroll, M. T. *Polyhedron* **1991**, *10*, 1247.

(16) (a) Nagase, S.; Kudo, T. *Organometallics* **1988**, *7*, 2534. (b) Kabe, Y.; Kawase, T.; Okada, J. *Angew. Chem., Int. Ed. Engl.* **1990**, *29*, 794. (c) Sita, L. R.; Kinnshita, I. *J. Am. Chem. Soc.* **1990**, *112*, 8839. (d) Veith, M.; Rösler, R. *Angew. Chem.* **1982**, *94*, 867; *Angew. Chem., Int. Ed. Engl.* **1982**, *21*, 858. (e) Veith, M.; Kunze, K. *Angew. Chem., Int. Ed. Engl.* **1991**, *30*, 95.

(17) Foster, J. M.; Boys, S. F. *Rev. Mod. Phys.* **1963**, *32*, 300.

(18) Gordon, M. S.; Packwood, T. J.; Carroll, M. T.; Boatz, J. A. *J. Phys. Chem.* **1991**, *95*, 4332.

(19) (a) Gordon, M. S.; Carroll, M. T.; Jensen, J.; Davis, L. P.; Burggraf, L. W.; Guidry, M. *Organometallics*, in press. (b) Schmidt, M. W.; Nguyen, K. A.; Gordon, M. S.; Montgomery, J. A., Jr. *J. Am. Chem. Soc.* **1991**, *113*, 5998.

(20) (a) Hehre, W. J.; Ditchfield, R.; Pople, J. A. *J. Chem. Phys.* **1971**, *51*, 2257. (b) Gordon, M. S. *Chem. Phys. Lett.* **1980**, *76*, 163. (c) Hariharon, P. C.; Pople, J. A. *Theor. Chim. Acta* **1973**, *28*, 213.

(21) Roothaan, C. C. J. *Rev. Mod. Phys.* **1951**, *23*, 69.

(22) Hsu, H.; Davidson, E. R.; Pitzer, R. M. *J. Chem. Phys.* **1976**, *65*, 609.

(23) Goddard, W. A., III; Dunning, T. H.; Hunt, W. J.; Hay, P. J. *Acc. Chem. Res.* **1973**, *6*, 368.

(24) Kahn, L. R.; Baybutt, P.; Truhlar, D. G. *J. Chem. Phys.* **1976**, *65*, 3826.

(25) Stevens, W. J.; Basch, H.; Krauss, M. *J. Chem. Phys.* **1984**, *81*, 6026.

**Table I.** Geometries and Energies ($E$(SCF) in hartrees, $E$(ZPE) in kcal mol$^{-1}$) of $M_2L_3$ (M = C, Si; L = O, S) Systems[a]

| systems | wave function | basis set | $E$(SCF) | $E$(ZPE) | distances, Å | | angles, deg | |
|---|---|---|---|---|---|---|---|---|
| | | | | | M–M | M–L | M–M–L | M–L–M |
| $C_2O_3$ | RHF | *a* | −300.042 60 | 11.7 | 1.456 | 1.393 | 58.5 | 60.0 |
| | | *b* | −57.790 64 | 11.6 | 1.481 | 1.405 | 58.2 | 63.6 |
| | ROHF | *a* | −299.990 56 | 12.7 | 1.561 | 1.415 | 56.5 | 67.0 |
| | | *b* | −57.738 89 | 12.7 | 1.581 | 1.425 | 56.3 | 67.4 |
| | TCSCF | *a* | −300.094 61 | 13.0 | 1.487 | 1.397 | 57.8 | 64.3 |
| | | *b* | −57.842 60 | 12.9 | 1.511 | 1.408 | 57.6 | 64.9 |
| $C_2S_3$ | RHF | *a* | −1 268.083 84 | 9.0 | 1.524 | 1.779 | 64.6 | 50.7 |
| | | *b* | −40.607 22 | 9.0 | 1.551 | 1.785 | 64.2 | 51.5 |
| | ROHF | *a* | −1 267.978 86 | 8.2 | 1.937 | 1.848 | 58.4 | 63.2 |
| | | *b* | −40.503 48 | 8.5 | 1.935 | 1.848 | 58.4 | 63.2 |
| | TCSCF | *a* | −1 268.111 07 | 8.8 | 1.616 | 1.786 | 63.1 | 53.8 |
| | | *b* | −40.635 64 | 8.9 | 1.640 | 1.792 | 62.8 | 54.5 |
| $Si_2O_3$ | RHF | *a* | −802.402 06 | 7.9 | 2.096 | 1.720 | 52.4 | 75.1 |
| | | *b* | −54.586 36 | 8.0 | 2.088 | 1.716 | 52.5 | 75.0 |
| | ROHF | *a* | −802.426 94 | 9.1 | 2.078 | 1.711 | 52.6 | 74.8 |
| | | *b* | −54.610 42 | 9.1 | 2.071 | 1.707 | 52.7 | 74.7 |
| | TCSCF | *a* | −802.459 25 | 9.1 | 2.084 | 1.711 | 52.5 | 75.0 |
| | | *b* | −54.643 46 | 9.1 | 2.076 | 1.707 | 52.6 | 74.9 |
| $Si_2S_3$ | RHF | *a* | −1 770.419 00 | 5.1 | 2.347 | 2.117 | 57.4 | 65.3 |
| | | *b* | −37.368 38 | 5.2 | 2.356 | 2.182 | 57.3 | 65.3 |
| | ROHF | *a* | −1 770.400 68 | 5.4 | 2.360 | 2.192 | 57.4 | 65.1 |
| | | *b* | −37.349 04 | 5.5 | 2.366 | 2.197 | 57.4 | 65.2 |
| | TCSCF | *a* | −1 770.454 09 | 6.0 | 2.357 | 2.176 | 57.2 | 65.6 |
| | | *b* | −37.403 28 | 6.0 | 2.363 | 2.180 | 57.2 | 65.6 |
| $Ge_2O_3$ | RHF | *b* | −54.441 86 | 6.3 | 2.269 | 1.817 | 51.4 | 77.2 |
| | ROHF | *b* | −54.434 81 | 7.1 | 2.233 | 1.807 | 51.8 | 76.3 |
| | TCSCF | *b* | −54.481 66 | 7.1 | 2.250 | 1.806 | 51.5 | 77.1 |
| $Sn_2O_3$ | RHF | *b* | −53.564 79 | 5.6 | 2.600 | 1.998 | 49.4 | 81.2 |
| | ROHF | *b* | −53.566 32 | 6.2 | 2.556 | 1.984 | 49.9 | 80.2 |
| | TCSCF | *b* | −53.601 42 | 6.2 | 2.577 | 1.985 | 49.5 | 81.0 |

[a] 6-31G(d). [b] SBK(d).

**Table II.** Geometries and RHF Energies ($E$(SCF) in hartrees, $E$(ZPE) in kcal mol$^{-1}$) of $M_2L_3H_2$ (M = C, Si, Ge, Sn; L = O, S) Systems

| system | basis set | $E$(SCF) | $E$(ZPE) | distances, Å | | | angles, deg | | |
|---|---|---|---|---|---|---|---|---|---|
| | | | | M–M | M–L | M–H | M–M–L | M–L–M | L–M–H |
| $C_2O_3H_2$ | *a* | −301.325 84 | 30.3 | 1.601 | 1.417 | 1.073 | 55.6 | 68.8 | 124.4 |
| | *b* | −59.076 98 | 30.3 | 1.622 | 1.427 | 1.077 | 55.4 | 69.3 | 124.3 |
| $C_2S_3H_2$ | *a* | −1 269.305 04 | 25.0 | 2.023 | 1.846 | 1.076 | 56.8 | 66.4 | 123.2 |
| | *b* | −41.827 28 | 25.4 | 2.020 | 1.846 | 1.080 | 56.8 | 66.3 | 123.2 |
| $Si_2O_3H_2$ | *a* | −803.683 72 | 21.0 | 2.067 | 1.703 | 1.452 | 56.7 | 74.7 | 127.3 |
| | *b* | −55.867 94 | 21.0 | 2.060 | 1.700 | 1.452 | 52.7 | 74.6 | 127.3 |
| $Si_2S_3H_2$ | *a* | −1 771.642 43 | 16.9 | 2.363 | 2.176 | 1.462 | 57.1 | 65.8 | 122.9 |
| | *b* | −38.591 01 | 16.9 | 2.373 | 2.181 | 1.464 | 57.0 | 65.9 | 123.0 |
| $Ge_2O_3H_2$ | *b* | −55.662 31 | 18.2 | 2.225 | 1.795 | 1.499 | 51.7 | 76.6 | 128.3 |
| $Sn_2O_3H_2$ | *b* | −54.757 28 | 15.8 | 2.546 | 1.971 | 1.668 | 49.8 | 80.5 | 130.0 |

[a] 6-31G(d). [b] SBK(d).

The nature of the bonding in the compounds of interest has been investigated with use of the electron density analysis developed by Bader and co-workers[12,27,28] as part of their theory of atoms in molecules. It has been found necessary to include an additional set of d functions on the M atoms to eliminate spurious non-nuclear maxima in the total charge density.[29] In the present work, the d orbital exponents used for this purpose are 1.6000, 0.4000 (C), 0.7900, 0.1975 (Si), 1.6000, 0.4000 (O), and 1.3000, 0.3250 (S). The density analysis has been discussed in detail elsewhere,[12,27,28] and only a few key points will be given here. A critical point in the charge density is a point at which the gradient of the charge density vanishes ($\nabla\rho(r) = 0$). A bond critical point ($r_b$) exists between two atoms if there is a saddle point in the electron density $\rho(r)$ between the two atoms. At this point the hessian of $\rho(r)$ has one positive eigenvalue along the bond axis and two negative eigenvalues along the axes orthogonal to the bond axis. The existence of a bond critical point implies the existence of a bond path (a line linking the two nuclei along which charge density is a maximum with respect to any lateral displacement) and the two atoms are said to be bonded. The hessian at a ring critical point ($r_r$) has two positive and one negative eigenvalues, with the density $\rho(r_r)$ at the ring critical point being smaller than that at all of the surrounding bond critical points. The hessian at a cage critical point has three positive curvatures and $\rho(r)$ is a local minimum at this point. If an $M_b$–$M_b$ bond is present in a [1.1.1]propellane system, one expects a bond critical point between the two bridgehead atoms, as well as three ring critical points, one on the face of each three-membered ring. The absence of such a bond critical point suggests that there is no "formal bond" connecting these two atoms.[12,27,28] However, such arguments may not reflect the existence of very flat electron density surfaces.[15]

## III. Results and Discussion

**A. Carbon and Silicon Compounds.** The RHF, ROHF, and TCSCF geometries of the propellanes **3** and RHF geometries of the bicyclopentanes **4** are listed in Tables I and II. Both all-electron and ECP calculations were carried out for M = C, Si and L = O, S. At all levels of theory (RHF, ROHF, and TCSCF), ECP bond lengths are within 0.02 Å of the 6-31G(d) all-electron calculations; bond angles agree to within a degree. Thus, as noted

---

(26) Schmidt, M. W.; Baldridge, K. K.; Boatz, J. A.; Jensen, J. H.; Koseki, S.; Gordon, M. S.; Nguyen, K. A.; Windus, T. L.; Elbert, S. T. *QCPE Bulletin, GAMESS, Indiana University* **1990**, *10*, 52.

(27) Bader, R. F. W.; Nguyen-Dang, T. T. *Adv. Quantum Chem.* **1981**, *14*, 63.

(28) Bader, R. F. W. *Acc. Chem. Res.* **1985**, *18*, 9.

(29) Boatz, J. A.; Gordon, M. S. *J. Phys. Chem.* **1989**, *93*, 3025.

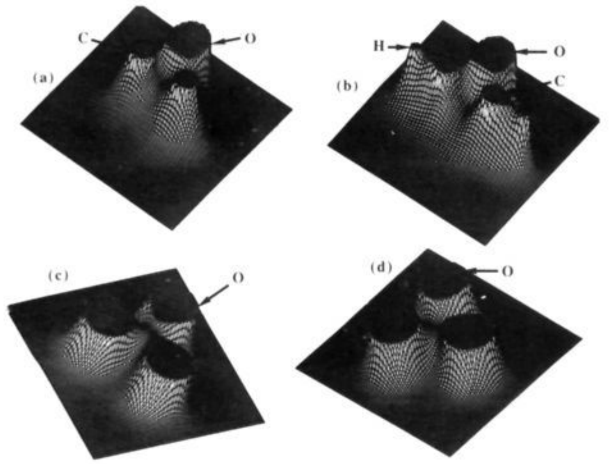

**Figure 1**. Relief maps of the charge distributions of $C_2O_3$ (a, c) and $C_2O_3H_2$ (b, d) systems in the $\sigma_v$ (a, b) and $\sigma_h$ (c, d) planes using the TCSCF/6-31G(2d)//TCSCF/6-31G(d) with the charge density cutoff of 0.32 and 0.22 au for the $\sigma_v$ and $\sigma_h$ planes, respectively. These maps are very similar in form to those generated by using the RHF/6-31G-(2d)//RHF/6-31G(d) wave functions.

earlier,[15] the ECP wave functions provide a consistently reasonable description of complex molecular geometries.

At the RHF/6-31G(d) level, the $M_b$–$M_b$ bridgehead distance in **3** (M = C, L = O) is only 0.09 Å shorter than the bridgehead distance of 1.543 Å in [1.1.1]propellane.[1] In contrast, the analogous difference is 0.60 Å when M = Si. As discussed earlier by Nagase and co-workers,[13b] the 2.096 Å bridgehead Si–Si distance in **3** is in fact much shorter than the 2.353 Å single Si–Si bond distance in disilane[30] and is actually less than the 2.143 double Si=Si bond distance in disilene.[31] The bonding of **3** (M = Si, L = O) was therefore explained in terms of a $\pi$-complex model,[32] with each peripheral oxygen and two bridgehead silicon atoms forming a T-shaped structure instead of a conventional three-membered ring. This assertion was based solely on the RHF bond distances and not on an analysis of electron density. In the sulfur analogues (Table I), the RHF/6-31G(d) C–C bridgehead distance (1.551 Å) is similar to that of [1.1.1]propellane (1.543 Å). In **3** (M = Si, L = S), the RHF/6-31G(d) Si–Si bridgehead distance (2.356 Å) is within the normal range of single Si–Si bond distances; however, this is still considerably shorter than the Si–Si bridgehead (2.719 Å) distance in pentasila[1.1.1]propellane.[10]

Thus, for M = Si, the M–M bridgehead distances in both the trioxa and trithia compounds **3** are predicted to be much shorter than the corresponding distances in the parent propellanes **1**, at the RHF level of theory. This raises two questions: (1) Do the shorter M–M bond distances correspond to stronger bonding interactions? (2) Are RHF wave functions adequate to describe these species? With regard to the former point, the geometry of compound **3** (with M = C, Si and L = O) may be highly constrained by the peripheral atoms in order to maintain the strong C–O and Si–O interactions and minimize O–O repulsions. Support for this is provided by noting that, in general, no significant increase is found in the M–M distances upon hydrogen additions at the bridgehead positions to form the corresponding bicyclopentane (**4**: M = C, L = O) systems (Table II). This suggests that either there are very strong M–M bonding interactions in *both* oxo derivatives (**3** and **4**) or there is little M–M bonding in **3** and no formal bridgehead bond in **4** with L = O. The latter would mean that the shorter bridgehead distance in these systems, relative to L = M, could simply be a result of geometrical constraint. Indeed, the geometries of the sulfur analogues of **3** and **4** reinforce exactly that interpretation. Furthermore, the C–C bond critical point (L = O) almost coalesces with the surrounding ring critical points, implying that a very flat distribution of charge in this central region (Figure 1). When L = S, however, the distribution is not as flat (Figure 2); the magnitude of the charge density $\rho(r)$ at the bond critical point is much larger than that at the surrounding ring critical points. This difference in $\rho(r)$ (between the bond critical point and ring critical point) when L = S is an order of magnitude larger than when L = O.

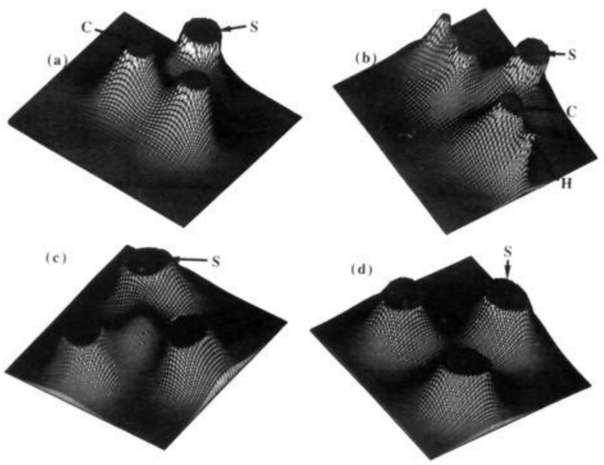

**Figure 2**. Relief maps of the charge distributions of $C_2S_3$ (a, c) and $C_2S_3H_2$ (b, d) systems in the $\sigma_v$ (a, b) and $\sigma_h$ (c, d) planes using the TCSCF/6-31G(2d)//TCSCF/6-31G(d) with the charge density cutoff of 0.32 and 0.22 au for the $\sigma_v$ and $\sigma_h$ planes, respectively. These maps are very similar in form to those generated by using the RHF/6-31G-(2d)//RHF/6-31G(d) wave functions.

**Table III**. TCSCF Coefficients and Natural Orbital Occupation Numbers (NOON) for $M_2O_3$ and $M_2S_3$ Systems

| systems | basis set | TCSCF coeff HOMO | TCSCF coeff LUMO | NOON HOMO | NOON LUMO |
|---|---|---|---|---|---|
| $C_2O_3$ | *a* | 0.954 | −0.300 | 1.820 | 0.179 |
|  | *b* | 0.934 | −0.301 | 1.819 | 0.181 |
| $C_2S_3$ | *a* | 0.978 | −0.207 | 1.914 | 0.086 |
|  | *b* | 0.977 | −0.212 | 1.910 | 0.090 |
| $Si_2O_3$ | *a* | 0.905 | −0.426 | 1.637 | 0.363 |
|  | *b* | 0.906 | −0.424 | 1.640 | 0.360 |
| $Si_2S_3$ | *a* | 0.946 | −0.324 | 1.790 | 0.210 |
|  | *b* | 0.947 | −0.323 | 1.792 | 0.208 |
| $Ge_2O_3$ | *b* | 0.936 | −0.352 | 1.752 | 0.248 |
| $Sn_2O_3$ | *b* | 0.928 | −0.372 | 1.724 | 0.276 |

[a] 6-31G(d). [b] SBK(d).

To assess the reliability of the RHF description of these compounds, TCSCF calculations were performed on the singlet states of **3**. This leads to two interesting results. First (Table I), TCSCF has little effect on the M–M distances, except in the case of **3** (M = C, L = S), where the TCSCF C–C bridgehead distance lengthens compared to the RHF value with the same basis set. Second, the TCSCF natural orbital occupation numbers (NOON) listed in Table III are quite large. The NOON are a convenient measure of the percent diradical character. The silicon derivative **3** (M = Si, L = O) has the highest percent diradical character (36%). The analogous value for the corresponding carbon compound is 18%. In contrast, the diradical character in [1.1.1]-propellane **1** is 10% for $M_b = M_p$ = C and 14% for $M_b = M_p$ = Si, at the same levels of theory.[15] The larger diradical character in **3** than in **1** diminishes the utility of interpretation based on RHF wave functions. The percent diradical character of **3** when M = C and L = S (9%) is almost identical with that of the parent propellane; the corresponding value (21%) for the silicon analogue (M = Si, L = S) is significantly larger than that of pentasilapropellane **1** ($M_p = M_b$ = Si). Thus, going from C to Si, the

---

(30) Francl, M. M.; Pietro, W. J.; Hehre, W. J.; Binkley, J. S.; Gordon, M. S.; DeFrees, D. J.; Pople, J. A. *J. Chem. Phys.* **1982**, *77*, 3654.

(31) Krogh-Jespersen, K. *J. Phys. Chem.* **1982**, *86*, 1492.

(32) (a) Dewar, M. J. S.; Ford, G. P. *J. Am. Chem. Soc.* **1979**, *101*, 783. (b) Cremer, D.; Kraka, E. *J. Am. Chem. Soc.* **1985**, *107*, 3800.

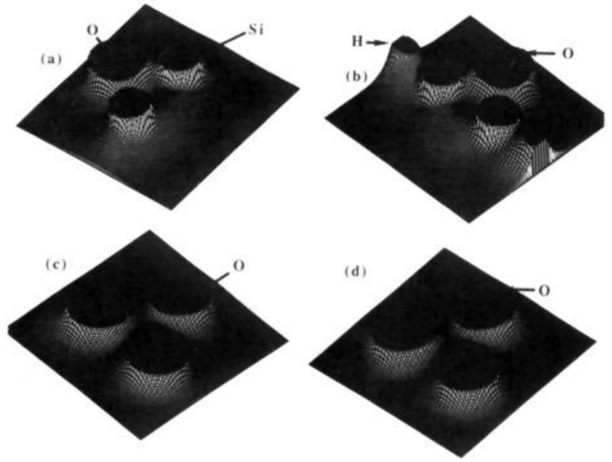

**Figure 3.** Relief maps of the charge distributions of $Si_2O_3$ (a, c) and $Si_2O_3H_2$ (b, d) systems in the $\sigma_v$ (a, b) and $\sigma_h$ (c, d) planes using the TCSCF/6-31G(2d)//TCSCF/6-31G(d) with the charge density cutoff 0.15 and 0.10 au for the $\sigma_v$ and $\sigma_h$ planes, respectively.

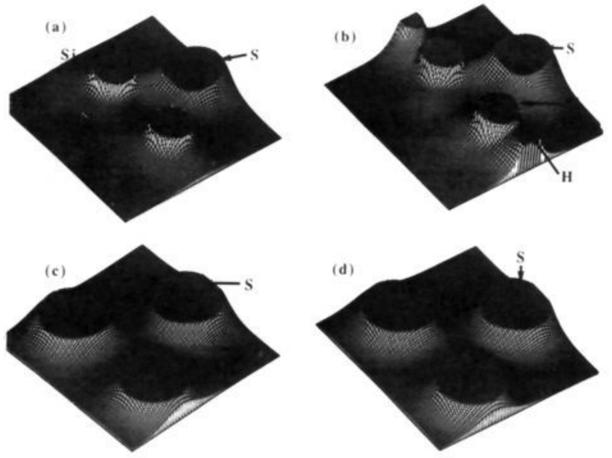

**Figure 4.** Relief maps of the charge distributions of $Si_2S_3$ (a, c) and $Si_2S_3H_2$ (b, d) systems in the $\sigma_v$ (a, b) and $\sigma_h$ (c, d) planes using the TCSCF/6-31G(2d)//TCSCF/6-31G(d) with the charge density cutoff of 0.15 and 0.10 au for the $\sigma_v$ and $\sigma_h$ planes, respectively.

**Table IV.** Singlet–Triplet Splittings for $M_2L_3$ (M = C, Si; L = O, S) Systems

| | $\Delta E$, kcal-mol$^{-1}$ (TCSCF-ROHF) | | | $\Delta E$, kcal-mol$^{-1}$ (TCSCF-ROHF) | |
|---|---|---|---|---|---|
| system | 6-31G(d) | SBK(d) | system | 6-31G(d) | SBK(d) |
| $C_2O_3$ | 65.3 | 65.0 | $Si_2S_3$ | 33.5 | 34.0 |
| $C_2S_3$ | 83.0 | 82.9 | $Ge_2O_3$ | | 29.4 |
| $Si_2O_3$ | 20.3 | 20.7 | $Sn_2O_3$ | | 22.0 |

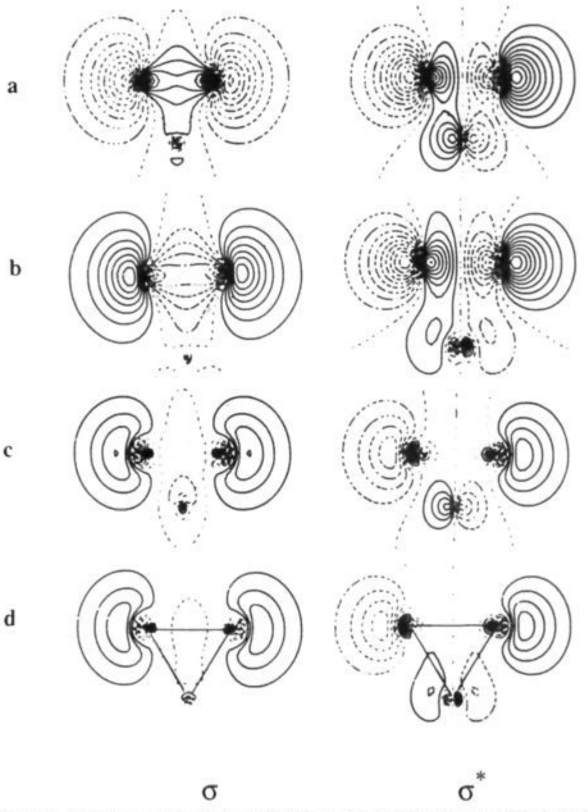

**Figure 5.** Contour plots of the HOMO and LUMO orbitals of $C_2O_3$ (a), $C_2S_3$ (b), $Si_2O_3$ (c), and $Si_2S_3$ (d) using TCSCF/6-31G(2d)//TCSCF/6-31G(d) wave functions.

percent diradical character approximately doubles for both the sulfur and oxygen propellane derivatives. The percent diradical character values obtained from all-electron calculations for carbon and silicon with L = O and S using the 6-31G(d) basis sets are essentially identical with those predicted by ECP.

Having established the importance of TCSCF descriptions of these systems, it is useful to analyze the total charge density derived from these wave functions. Figures 1–4 display relief maps of the total charge density in both the $\sigma_h$ (containing the three peripheral atoms (L) in **3** and **4**) and the $\sigma_v$ (containing one peripheral atom (L) and two bridgehead atoms (M) in **3** and **4**) planes. Since the $\sigma_h$ plane bisects the bridgehead M–M axes, any concentration of charge density [$\rho(r)$] in the bridgehead regions will produce a bump. Accumulation of charge density in the bridgehead regions in the $\sigma_v$ plane will only produce a saddle, since $\rho(r)$ at nuclei are always greater than $\rho(r)$ in bonding and nonbonding regions. For both carbon propellane derivatives, there is a significant accumulation of charge between the two carbon nuclei. Indeed, a bond critical point is located (as was the case for the parent propellane). However, in the bicyclopentane compounds, there is relatively little charge density distributed in the bridgehead regions.

In the silicon propellane derivatives, the distribution of electron density in the bridgehead region is flat (Figure 3 and 4). The fact that there is little charge accumulated between the two silicon nuclei and more charge accumulated along the Si–O and Si–S bonds does not support the proposal[13b] of a T-shaped bonding mechanism for the pentasilapropellane trioxa and trithia derivatives. Also, note that addition of two hydrogens across the bridgehead does not result in any significant change in the amount of charge density between the bridgehead silicons (Figures 3 and 4). No Si–Si bond critical point is found in these silicon compounds.

Further evidence for the large diradical character in **3** is provided by ROHF calculations on the corresponding triplet states, obtained via an excitation of one electron from the M–M bonding orbital ($\sigma$) to its antibonding MO ($\sigma^*$). The singlet–triplet splittings for these species are compiled in Table IV. Note the good agreement between all-electron and ECP methods and also that the singlet is more stable than the triplet in all cases. Further, replacement of O by S leads to a stabilization of the singlet over the triplet by 17.7 kcal/mol for M = C and 13.3 kcal/mol for M = Si. This is consistent with the greater diradical character found in the oxo than in the thia compounds. Thus, it is seen that as the L group (L = O and S) decreases in electronegativity relative to M (M = C and Si), the closed-shell character of the system increases. Not unexpectedly, inspection of the HOMO and LUMO plots (Figure 5) shows that in the bridgehead region, the electron density is polarized to a greater extent toward the peripheral atoms as the electronegativity of L increases. This apparently results in a smaller singlet–triplet splitting for L = O. The more electronegative oxygen polarizes electron density to a greater extent than does sulfur. These observations suggest that except for 2,4,5-trithia[1.1.1]propellane, single determinant wave function treatments may not be appropriate for these species.

**B. Germanium and Tin Compounds.** Since ECP calculations compare favorably with full ab initio results, only ECP results are reported for the heavier atoms. The most interesting electronic structural features found for C and Si are those in the trioxa species, so we limit ourselves to these and omit discussion of the sulfur analogues. The results of structures, energetics, and the TCSCF NOON of the germanium and tin trioxa[1.1.1]propellane derivatives are listed in Tables I–IV along with the carbon and silicon analogues. Because the essential conclusions drawn for Ge and Sn compounds (**3** and **4** with M = Ge, Sn and L = O) are the same as those discussed above for C and Si, only the key features of these species will be addressed.

In both the germanium and tin analogues of **3** (L = O) extremely short bridgehead M–M distances are found at the RHF, ROHF, and TCSCF levels of theory. These bridgehead M–M distances are not significantly affected by the additions of hydrogens across the bridgehead centers (cf. Tables I and II). Indeed, the differences between the M–M distances in the propellanes **3** and the bicyclopentane **4** analogues are less than 0.1 Å for both M = Ge and Sn. Furthermore, differences among the three levels of theory (RHF, ROHF, and TCSCF) in the corresponding M–M bridgehead distances are within 0.1 Å. These results are similar to those found in the silicon analogues of **3** and **4**. The RHF/SBK(d) geometric results for **3** (M = Ge, L = O) and the corresponding bicyclopentane analogue are essentially identical with those calculated by Nagase and Kudo[13a] using the 3-21G(d) basis set at the RHF level of theory. The percent diradical character and the singlet–triplet splittings for Sn (28%, 22.0 kcal mol$^{-1}$) and Ge (25%, 29 kcal mol$^{-1}$) are also similar to those discussed above (36%, 20.7 kcal mol$^{-1}$) for the Si analogue of **3**.

## IV. **Conclusions**

In this study, ab initio molecular orbital theory has been used to investigate the structure and bonding of sulfur and oxygen propellane derivatives (**3**) and their bicyclopentane analogues (**4**) with RHF, ROHF, and TCSCF wave functions. We have found that the M = Si, Ge, and Sn species possess unusually short bridgehead distances. However, this does not result in significant bonding interactions, as shown by the TCSCF calculations and total density plots. For M = C, TCSCF calculations and total density analyses suggest substantial bridgehead bonding only in the L = S system. We have found excellent agreement in structures and energetics between ECP calculations and the 6-31G(d) all-electron calculations.

**Acknowledgment.** The computations described in this work were performed on the North Dakota State University IBM 3090/200E vector computer, obtained in part with the aid of a joint study agreement between IBM and NDSU, and on the Cray-2 at the National Center for Supercomputing Applications, Champaign, Illinois. This work was supported in part by a grant from the National Science Foundation (CHE-8911911). We thank Walter Stevens, Morris Krauss, Harold Basch, and Paul Jasien for making their ECPs available to us prior to publication.

---

# Rotational Energy Surfaces of Aza- and Phospha-1,3-butadienes. A Theoretical Study

**Steven M. Bachrach* and Meixiao Liu**

*Contribution from the Department of Chemistry, Northern Illinois University, DeKalb, Illinois 60115.* *Received April 15, 1991*

**Abstract:** The rotational energy surfaces of all stereoisomers of 1-aza-, 2-aza-, 1,3-diaza-, 1,4-diaza-, and 2,3-diaza-1,3-butadienes and 1-phospha-, 2-phospha-, 1,3-diphospha-, 1,4-diphospha-, and 2,3-diphospha-1,3-butadienes were calculated at the MP2/6-31G*//HF/6-31G* level. Rotational barriers and all local minima were rigorously located and identified. For all systems except *anti*-1,3-diaza-1,3-butadiene, the *trans* conformer is the global minimum. Stable *gauche* isomers are present for most azabutadienes and all phosphabutadienes. Rotational barriers for the azabutadienes are between 1.4 and 8.6 kcal mol$^{-1}$ and between 3.1 and 8.1 kcal mol$^{-1}$ for the phosphabutadienes. The shapes and relative heights of the critical points on the rotational surfaces are discussed in terms of $\pi$-delocalization, 1,4-steric interactions, and intramolecular hydrogen bonding. The low rotational barriers and stable *gauge* conformers of the phosphabutadienes indicate that these molecules should undergo electrocyclic and cycloaddition reactions that require *cis*-like conformations of the diene.

Although the degree of delocalization of $\pi$-electrons through conjugation is a matter of some controversy,[1] the conformational preference for extended planar systems does support its existence. Both experimental[2–8] and theoretical[9–15] studies conclude that the lowest energy conformation is planar with an *s-trans* arrangement about the C–C single bond. The nature of the second stable conformer, about 2.5–4.0 kcal mol$^{-1}$ higher in energy, is disputed. IR[5] and Raman[2] spectroscopy suggest a cis planar minimum,

---

(1) Popov, E. M.; Kogan, G. A. *Russ. Chem. Rev.* **1968**, *37*, 119–141.

(2) Carreira, L. A. *J. Chem. Phys.* **1975**, *62*, 3851–3854.

(3) Durig, J. R.; Bucy, W. E.; Cole, A. R. H. *Can. J. Phys.* **1975**, *53*, 1832–1837.

(4) Squillacote, M. E.; Sheridan, R. S.; Chapman, O. L.; Anet, F. A. L. *J. Am. Chem. Soc.* **1979**, *101*, 3657–3659.

(5) Furukawa, Y.; Takeuchi, H.; Harada, I.; Tasumi, M. *Bull. Chem. Soc. Jpn.* **1983**, *56*, 392–399.

(6) Squillacote, M. E.; Semple, T. C.; Mui, P. W. *J. Am. Chem. Soc.* **1985**, *107*, 6842–6846.

(7) Fischer, J. J.; Michl, J. *J. Am. Chem. Soc.* **1987**, *109*, 1056–1059.

(8) Arnold, B. R.; Balaji, V.; Michl, J. *J. Am. Chem. Soc.* **1990**, *112*, 1808–1812.

(9) Breulet, J.; Lee, T. J.; Schaefer, H. F., III *J. Am. Chem. Soc.* **1984**, *106*, 6250–6253.

(10) Bock, C. W.; George, P.; Trachtman, M. *Theor. Chim. Acta* **1984**, *64*, 293–311.

(11) De Mare, G. R.; Neisius, D. *J. Mol. Struct.* (*THEOCHEM*) **1984**, *109*, 103–126.

(12) Rice, J. E.; Liu, B.; Lee, T. J.; Rohlfing, C. M. *Chem. Phys. Lett.* **1989**, *161*, 277–284.

(13) Bock, C. W.; Panchenko, Y. N. *J. Mol. Struct.* (*THEOCHEM*) **1989**, *187*, 69–82.

(14) Wiberg, K. B.; Rosenberg, R. E. *J. Am. Chem. Soc.* **1990**, *112*, 1509–1519.

(15) Guo, H.; Karplus, M. *J. Chem. Phys.* **1991**, *94*, 3679–3699.

0002-7863/91/1513-7929$02.50/0